THE JOURNAL OF PHYSICAL CHEMISTRY B

Article

pubs.acs.org/JPCB

Molecular Modeling of Fluoropropene Refrigerants

Gabriele Raabe*

Institut für Thermodynamik, Technische Universität Braunschweig, Hans-Sommer-Str. 5, 38106 Braunschweig, Germany

Supporting Information

ABSTRACT: Different fluoropropenes are currently considered as refrigerants, either as pure compounds or as components in low GWP (global warming potential) refrigerant mixtures. Due to their limited commercial production, experimental data for the thermophysical properties of fluoropropenes and their mixtures are in general rare, which hampers the exploration of their performance in technical applications. In principle, molecular simulation can be used to predict the relevant properties of refrigerants and refrigerant blends, provided that adequate intermolecular potential functions ("force fields") are available. In our earlier work (Raabe, G.; Maginn, E. J., *J. Phys. Chem. B* **2010**, *114*, 10133−10142), we introduced a transferable force field for fluoropropenes comprising the compounds 3,3,3-trifluoro-1-propene (HFO-1243zf), 2,3,3,3-tetrafluoro-1-propene (HFO-1234yf), and hexafluoro-1-propene (HFO-1216). In this paper, we provide an extension of the force field model to the trans- and cis-1,3,3,3-tetrafluoro-1-propene (HFO-1234ze(E), HFO-1234ze) and the cis-1,2,3,3,3-pentafluoro-1-propene (HFO-1225ye(Z)) as well as revised simulation results for HFO-1216. We present Gibbs ensemble simulation results on the vapor pressures, saturated densities, and heats of vaporization of these compounds in comparison with experimental results. The simulation results show that the force field model enables reliable predictions of the properties of the different fluoropropenes and also reproduces well the differing vapor−liquid coexistence and vapor pressure curve of the cis- and trans-isomers of 1,3,3,3-tetrafluoro-1-propene, HFO-1234ze and HFO-1234ze(E). For these two isomers, we also present molecular dynamics simulation studies on their local structure.

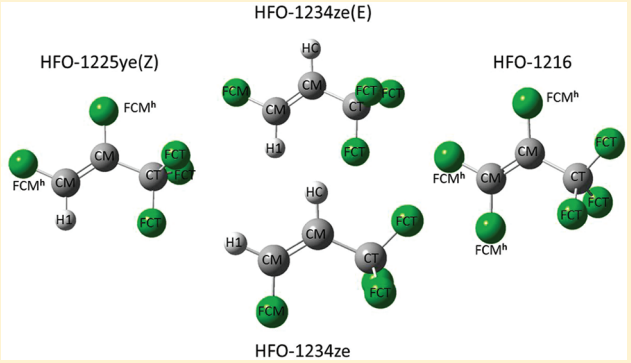

1. INTRODUCTION

Hydrofluorolefins (HFOs) in general and fluoropropene compounds in particular have lately attracted great attention as alternative refrigerants due to their low global warming potential (GWP). The compound HFO-1234yf (2,3,3,3-tetrafluoro-1-propene), for instance, is currently regarded as the most promising replacement for the high GWP refrigerant R134a (tetrafluoroethane) in mobile heating, ventilation, and air conditioning (HVAC) systems.[1,2] However, also other fluoropropene compounds are considered as refrigerants or are already utilized in various applications. The trans-1,3,3,3-tetrafluoro-1-propene HFO-1234ze(E), for instance, is used as an aerosol or foam blowing agent[3] but is also studied as a refrigerant, either as a pure compound[3,4] or in refrigerant mixtures.[5,6] The hexafluoropropene HFO-1216 is utilized as an intermediate and monomer in the fluorochemical industry[7] but is again also considered as a working fluid for refrigeration.[8] Beyond that, a large number of patents or patent applications propose the use of low GWP refrigerant mixtures as blends of HFOs and hydrofluorocarbons (HFC) (see, for instance, refs 9−14).

The exploration of the performance of these new refrigerants or possible refrigerant mixtures in technical applications requires a detailed knowledge of their thermodynamic and transport properties. Due to limited commercial production, experimental data for fluoropropenes in the literature are in general rare, and mainly comprise information on the compounds HFO-1234yf (see, for instance, refs 15−18) and HFO-1234ze(E).[3−5,19−21] For these two compounds, also accurate equations of state are available[3,22] in the NIST Standard Reference Database REFPROP.[23] Compared to this, only little information is available on the thermophysical properties of the other fluoropropenes, and generally for mixtures of the HFOs with other compounds.

In principle, molecular modeling can be used to predict the relevant properties of refrigerants and refrigerant blends, but adequate intermolecular potential functions ("force fields") have been missing for fluoropropenes. Thus, we intend to provide a transferable force field for fluorinated propenes that enables reliable predictions for the thermophysical and transport properties of this new class of alternative refrigerants and also of their mixtures by molecular simulation studies to complement experimental data. The fluoropropenes directly considered in the first state of our force field parametrization[24,25] have been 3,3,3-trifluoro-1-propene (HFO-1243zf), 2,3,3,3-tetrafluoro-1-propene (HFO-1234yf), and hexafluoro-1-propene (HFO-1216). In this paper, we provide an extension of the force field model to HFO-1234ze(E), HFO-1234ze (cis-

Received: January 31, 2012
Revised: April 20, 2012
Published: April 20, 2012

   dx.doi.org/10.1021/jp300991t | *J. Phys. Chem. B* 2012, 116, 5744−5751

1,3,3,3-tetrafluoro-1-propene), and cis-1,2,3,3,3-pentafluoro-1-propene HFO-1225ye(Z) as well as revised simulation results for HFO-1216. Furthermore, we present molecular dynamics simulation studies on the differences in the local ordering of the isomers HFO-1234ze and HFO-1234ze(E).

2. FORCE FIELD DEVELOPMENT

In our force field model, the potential energy of the fluoropropenes is expressed by the following standard functional form[26]

$$U_{\mathrm{Conf}} = \sum_{\mathrm{bonds}} k_r(r - r_0)^2 + \sum_{\mathrm{angles}} k_\theta(\theta - \theta_0)^2 + \sum_{\mathrm{dihedral}} k_\chi[1 + \cos(n\chi - \delta)] + \sum_i \sum_{j>i} \left\{ 4\varepsilon_{ij}\left[\left(\frac{\sigma_{ij}}{r_{ij}}\right)^{12} - \left(\frac{\sigma_{ij}}{r_{ij}}\right)^{6}\right] + \frac{1}{4\pi\varepsilon_0}\frac{q_i q_j}{r_{ij}} \right\} \quad (1)$$

Therein, the calculation of intermolecular interactions is based on site−site terms with Lennard-Jones interaction centers on the atomic sites and additional fixed partial charges to model the electrostatic interactions. The intramolecular potential energy is described by harmonic terms for bond stretching and angle bending, a cosine term to include energies arising from internal rotations of the dihedral angles, and nonbonded interactions between atoms separated by at least three bonds. Nonbonded Lennard-Jones (LJ) and electrostatic interactions between atoms separated by exactly three bonds (1−4 interactions) are scaled by a factor of 1/2 and 1/1.2, respectively. All LJ parameters for unlike atoms are obtained from the Lorentz−Berthelot combining rule.

The nominal bond lengths r_0 and bond angles θ_0 were obtained from quantum mechanical (QM) calculations to determine the energy minimized structure of an isolated molecule. The geometries have been optimized at the B3LYP[27,28]/DGDZVP[29] level of theory using the Gaussian 03 package.[30] We have then averaged the force field parameters for the nominal bond lengths r_0 and bond angles θ_0 to obtain a transferable force field with a reduced number of different parameters. The force constants for the bond stretching and angle bending were also derived from ab initio simulations by perturbing the bond length or angle around their equilibrium value. k_r and k_θ were then determined from the fitting of the harmonic potential to the resulting energy change versus the degree of perturbation. The parameters for the torsion potentials associated with the CM-CT bond were derived from torsion scanning calculations.

The partial charges were calculated for all compounds individually from ab initio simulations by the ESP approach with the CHELPG fitting scheme.[31] The electrostatic potentials have been determined for the isolated molecules whose geometries were optimized on the B3LYP/DGDZVP level of theory as described above. To account for polarization effects in the liquid phase, we computed the partial charges for isolated molecules at the HF/6-31G* level of theory.[30] The partial charges for the compounds newly covered in this work, i.e., HFO-1234ze, HFO-1234ze(E), and HFO-1225ye(Z), are summarized in Table 1. It is worth mentioning that the derived partial charges result in a much higher dipole moment of $\mu_{\mathrm{HFO\text{-}1234ze}}$ = 3.54 D for the cis-isomer HFO-1234ze compared to the value of $\mu_{\mathrm{HFO\text{-}1234ze(E)}}$ = 1.31 D for the trans-isomer.

Table 1. Partial Charges of the Fluoropropenes Studied in This Work[a]

	HFO-1234ze(E)		HFO-1234ze		HFO-1225ye(Z)	
#	type	q (e)	type	q (e)	type	q (e)
1	CM	0.25325	CM	0.23034	CM	0.07582
2	CM	−0.48504	CM	−0.52066	CM	0.05606
3	CT	0.77614	CT	0.98095	CT	0.53681
4	FCM	−0.19161	H1	0.13221	FCM[h]	−0.14148
5	H1	0.13249	FCM	−0.16993	H1	0.15570
6	HC	0.24464	HC	0.20221	FCM[h]	−0.12905
7	FCT	−0.24329	FCT	−0.28504	FCT	−0.18462
8	FCT	−0.24329	FCT	−0.28504	FCT	−0.18462
9	FCT	−0.24329	FCT	−0.28504	FCT	−0.18462

[a]The partial charges for HFO-1216 used in this work are the same as in our earlier work.[25]

The notation for the different Lennard-Jones atom types in our transferable force field is given in Figure 1. We used the atom type CM for the double bonded sp2 carbon and CT for the sp3 carbon, and have additionally introduced the atom types FCM and FCT for the fluorines bonded to the CM or CT carbon, respectively. The parameters for the HC hydrogen attached to the CM carbon in HFO-1234yf and HFO-1243zf (carbon with no electron-withdrawing substituents) were taken from the AMBER force field.[26] Consequently, we also used the AMBER H1 parameter for the hydrogen attached to CM with one electron-withdrawing substituent (FCM) in HFO-1234ze, -1234ze(E), and -1225ye(Z). All other LJ parameters were adjusted to fine-tune agreement with experimental data for selected compounds. Table 1 in the Supporting Information (jp300991t_si_001.pdf) provides an overview over which components were used to establish the LJ parameters for several atom types (CM, CT, FCT, FCM, FCM[h], HC, H1, HC1). Please note that, with the exception of the introduction of the AMBER H1 parameter, all LJ parameters used in the modeling of HFO-1234ze and -1234ze(E) are the same as those for HFO-1234yf; i.e., no LJ parameters were adjusted for these compounds. However, we found that the FCM parameter used to describe the compounds with up to four fluorines makes HFO-1225ye(Z) a too high-boiling compound. Thus, we derived a modified FCM[h] parameter for compounds with more than four fluorines, with which we then also revised our previous simulation results[25] for HFO-1216.

Regarding the description of the intramolecular potential energy, only the nominal bond angles θ_0 and the force constant k_θ for the bending of the angle H1-CM-FCM in the compounds HFO-1234ze, -1234ze(E), and -1225ye(Z) were derived in this work, whereas all other intramolecular potential parameters were taken from our earlier work.[25] That also means that we used the same parameters for the intramolecular terms including the FCM[h] and H1 atoms as we did for the FCM and HC atoms, respectively. We'd like to point out that the phase angles δ and multiplicities n in the torsion terms need to be assigned attentively to account for different equilibrium geometries of the fluoropropenes (regarding the CF_3 group, see Figure 1), and also to distinguish between conformational isomers. Tables 2 and 3 in the Supporting Information (jp300991t_si_001.pdf) give a detailed compilation of the parameter settings for δ and n in the different compounds. In the Supporting Information (jp300991t_si_001.pdf), we also

dx.doi.org/10.1021/jp300991t | J. Phys. Chem. B 2012, 116, 5744−5751

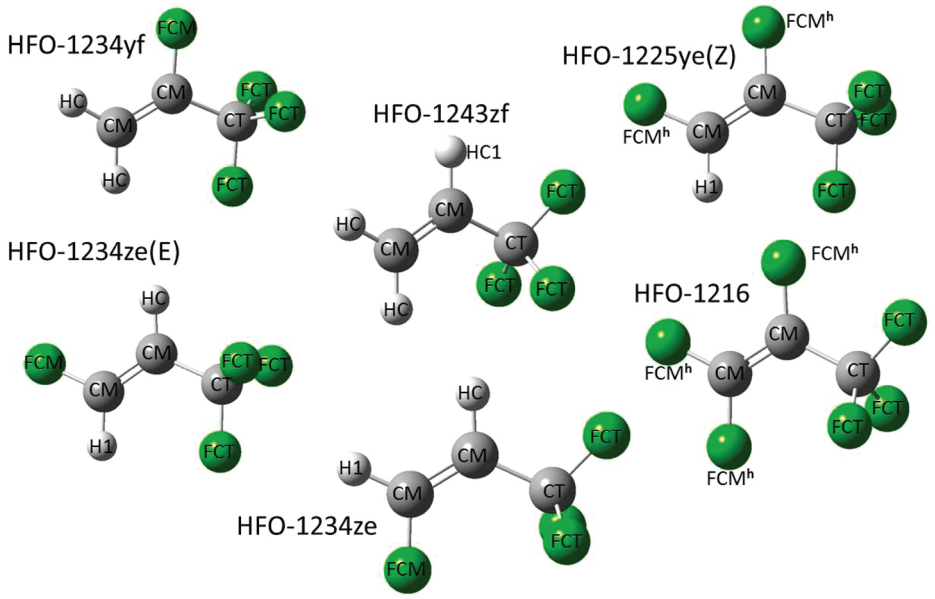

Figure 1. Structures of all the fluoropropenes currently covered by the force field: 3,3,3-trifluoropropene (HFO-1243zf), 2,3,3,3-tetrafluoropropene (HFO-1234yf), 1,1,2,3,3,3-hexafluoropropene (HFO-1216), trans-1,3,3,3-tetrafluoropropene (HFO-1234ze(E)), cis-1,3,3,3- tetrafluoropropene (HFO-1234ze), and cis-1,2,3,3,3-pentafluoropropene (HFO-1225ye(Z)), and nomenclature for the different atom types.

provide the complete set of force field parameters for the different fluoropropenes. For more details on the parametrization of the molecular model, we'd like to refer to our earlier work.[25]

3. SIMULATION DETAILS

Vapor−liquid coexistence curves were calculated via the Monte Carlo Gibbs ensemble[32] (GEMC) using the simulation code Towhee,[33] with systems consisting of 256 molecules. The Ewald sum technique[34,35] was employed to deal with the electrostatic interactions with a cutoff radius adjusted to half the box length. The cutoff radius for the Lennard-Jones interactions was set to 12 Å, and standard long-range corrections to the energy and pressure were applied.[35] The simulations were equilibrated for 100 000−200 000 cycles, followed by production runs of 200 000−300 000 cycles. Each cycle consisted of 256 attempted moves, such as a volume move, translation of the center-of-mass, rotation about the center-of-mass, and a configurational-bias exchange move[36] between the boxes. The moves were selected at random with a fixed probability. However, the probabilities of the different moves were manually adjusted for each temperature to ensure that the equilibrium conditions were satisfied, i.e., that the simulated chemical potentials in both phases agreed within the error bars.

The pressures were calculated via the pressure virial equation using the vapor phase. The heats of vaporization ΔH_{vap} were determined using the energy U and density ρ of the liquid and vapor phases and the vapor pressure p_s:

$$\Delta H_{vap} = U^V - U^L + p_s^V\left(\frac{1}{\rho^V} - \frac{1}{\rho^L}\right) \quad (2)$$

where the superscripts designate the simulation boxes, i.e., the saturated liquid and vapor phase.

Standard deviations of all ensemble averages were determined by the standard block average technique,[35] dividing the production runs into 10 blocks.

The critical temperatures T_c and densities ρ_c of the different compounds were estimated by fitting the simulation results at subcritical conditions to the scaling law[35]

$$\rho^L - \rho^V = A\tau^\beta \quad \text{with} \quad \tau = 1 - \frac{T}{T_C} \quad (3)$$

and the law of rectilinear diameters

$$\frac{\rho^L + \rho^V}{2} = \rho_c + B\tau \quad (4)$$

by employing the Towhee utility routine fitcoex.[33] We assumed the critical exponent to be $\beta = 0.32$.[35] The critical pressures p_c were estimated by extrapolating the vapor pressure curves using the Clausius−Clapeyron equation. This also yields an estimate of the normal boiling point T_b of the compounds. The stated errors of the critical properties and normal boiling point are those given by the fitcoex routine, and they account for both the uncertainties of the simulated properties as input data and the errors of the fitting procedure.

We have tested our approach to estimate T_c, ρ_c, p_c, and T_b by applying the fitcoex routine[33] with $\beta = 0.32$ to experimental data[8] for HFO-1216. We found that the estimated properties are in good agreement with the experimental data given by Coquelet et al.[8] We have additionally varied the critical exponent from $\beta = 0.32$ to 0.35. The deviations between the predicted values using different exponents β are smaller than our given uncertainties for the estimated critical properties, so that systematic errors due to uncertainties in β seem to be negligible.

We have additionally performed molecular dynamics (MD) simulations in the liquid phase for (cis) HFO-1234ze and (trans) HFO-1234ze(E) using the DL_POLY simulation package.[37] The cubic boxes consisted of $N = 216$ molecules, and periodic boundary conditions were applied. Again, the Ewald sum was used to deal with the electrostatic interactions. The cutoff radii for both the real space part of the Ewald sum and the LJ interactions were set to 14 Å, and standard long-

dx.doi.org/10.1021/jp300991t | J. Phys. Chem. B 2012, 116, 5744−5751

Table 2. Estimated Critical Properties and Normal Boiling Points of the Compounds Studied in This Work in Comparison with Experimental Data Where Available[a]

	$T_{c,sim}$ (K)	$T_{c,exp}$ (K)	$\rho_{c,sim}$ (kg m^{-3})	$\rho_{c,exp}$ (kg m^{-3})	$p_{c,sim}$ (MPa)	$p_{c,exp}$ (MPa)	$T_{b,sim}$ (K)	$T_{b,exp}$ (K)
HFO-1234yf	366.6 ± 9.5	367.9[b,c]	470 ± 26	478[c]	3.38 ± 0.73	3.26[b]−3.38[c]	243.3 ± 3.5	243.8[b]*
HFO-1243zf	375.5 ± 14.5	376.2[d]−380.8[e]	422 ± 40	455.22[d]−462.2[e]	3.56 ± 1.1	3.61[d]−3.79[e]	250.1 ± 4.3	249.3[e]
HFO-1216	364.3 ± 13.2	358.93[f]	590 ± 49	579.03[f]	3.34 ± 1.13	3.136[f]	242.4 ± 6.6	243.6[f]
HFO-1234ze(E)	381.4 ± 10.7	382.51[g]	487 ± 29	486[g]	3.87 ± 0.86	3.632[g]	254.9 ± 2.3	254.15
HFO-1234ze	417.9 ± 9.2	*426.8*[i]	457 ± 23	*473*[i]	3.34 ± 0.66	*3.970*[i]	283.6 ± 3.5	282.15[h]
HFO-1225ye(Z)	381.6 ± 15.7	378.2[e]	534 ± 43	527[e]	3.67 ± 1.15	3.183[e]	254.2 ± 3.1	253.5[e]

[a]Also given are the estimated properties of HFO-1234yf and HFO-1243zf derived in our earlier work.[25] [b]Hulse et al.;[15] * mark interpolated results. [c]Tanaka et al.[17] [d]Gmehling.[40] [e]Singh,[41] from fitting the experimental VLCC to the scaling law and the law of rectilinear diameters, $T_{b,exp}$ is interpolated. [f]Coquelet et al.[8] [g]Higashi et al.[4] [h]Mukhopadhyay et al.[42] [i]Brown et al.,[43] estimated data.

range corrections to the van der Waals interactions were applied. We performed simulations in the Nosé−Hoover[38,39] NpT ensemble, in which the trajectories were integrated by the velocity Verlet algorithm[35] with a time step of Δt = 0.0005 ps and coupling constants of τ_T = 0.1 ps and τ_p = 1.0 ps. The systems were equilibrated for 2.0 ns, followed by a production run of 5 ns, which was divided into 10 blocks to derive ensemble averages for the standard deviations. During the production run, we saved the configurations of HFO-1234ze and -1234ze(E) every 0.025 ps for the structural analysis of the conformational isomers by radial distribution functions (RDFs).

Due to the relatively small system size of both our GEMC and MD studies, we have performed additional test simulations with a larger number of molecules to check that our simulation results are not affected by system size effects. We found that the simulation results for different system sizes agree within the range of their uncertainties.

4. RESULTS AND DISCUSSION

Results from GEMC Simulations for Different Flouropropenes. The extension and revision of the force field has been tested by performing Gibbs ensemble simulations on the vapor liquid equilibrium (VLE) of 1,3,3,3-trifluoro-1-propene (cis- and trans-HFO-1234ze), cis-1,2,3,3,3-pentafluoro-1-propene (HFO-1225ye(Z)), and hexafluoro-1-propene (HFO-1216). In the following section, we discuss in detail the performance of the force field regarding the prediction of the vapor−liquid phase equilibria and critical properties of the fluoropropenes HFO-1234ze, HFO-1234ze(E), HFO-1225ye-(Z), and HFO-1216. Numerical results for the simulated vapor pressures, saturated densities, and heats of vaporization of these compounds are given as Supporting Information (jp300991t_si_002.pdf). In Table 2, we have summarized the predictions for the critical properties and normal boiling points of all compounds currently covered by the force field in comparison with available experimental data.[4,8,15,17,40−42]

Vapor−Liquid Equilibria of HFO-1234ze(E) and -1234ze. The modeling of intermolecular interactions for trans-HFO-1234ze(E) is based on individually determined partial charges, the Amber H1 parameter,[26] and LJ parameters derived in our previous work (see section 2). As no LJ parameters have been adjusted for this compound, the simulations for HFO-1234ze(E) are purely predictive. In spite of this, the agreement of simulation results for the vapor pressures and saturated densities with experimental data[4,19,20] is quite satisfying, as illustrated by Figures 2 and 3. The simulations though tend to overestimate the vapor pressures for temperatures above 290 K, whereas the simulated saturated liquid densities at low

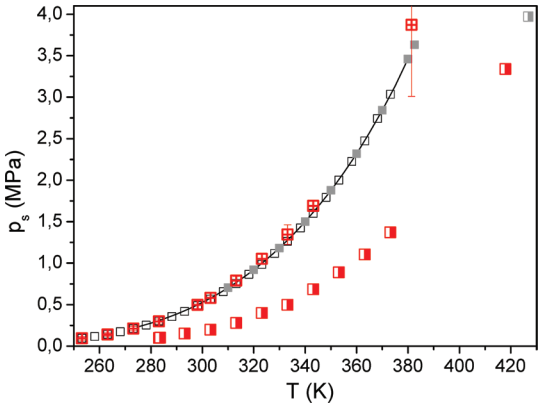

Figure 2. Gibbs ensemble simulation results for the vapor pressure of HFO-1234ze(E) (red ⊞) and HFO-1234ze (red ◨) obtained in this work. Also given are the experimental data for HFO-1234ze(E) (□,[19] gray ■[20]) and the calculated vapor pressure curve (solid line) using REFPROP.[23] The data point (gray ◨) is the estimated critical point of HFO-1234ze by Brown.[43]

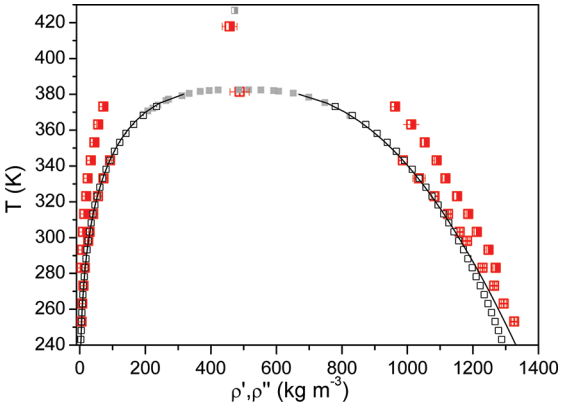

Figure 3. Comparison between experimental saturated liquid densities of HFO-1234ze(E) (□,[19] gray ■[20]) and Gibbs ensemble simulation results for the saturated densities (red ⊞) obtained in this work and calculation using REFPROP[23] (as solid line). Also given are the simulation results for HFO-1234ze (red ◨) and the estimated critical point (gray ◨) by Brown.[43]

temperatures are higher than both the experimental data and the REFPROP calculations.[21,23] Figure 4 reveals that the heats of vaporization of HFO-1234ze(E) are also overestimated by the simulation. However, to achieve a better agreement with experimental liquid densities and heats of vaporization, the interaction energies, i.e., the LJ parameters ε, need to be reduced, which in turn would result in even higher vapor

dx.doi.org/10.1021/jp300991t | J. Phys. Chem. B 2012, 116, 5744−5751

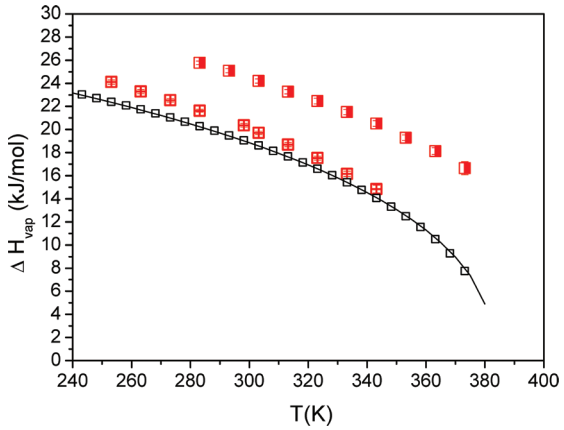

Figure 4. Gibbs ensemble simulation results for the heats of vaporization of HFO-1234ze(E) (red ⊞) and HFO-1234ze (red ◨) obtained in this work. Also shown are the experimental data for HFO-1234ze(E) (□[19]) and calculated $\Delta H_{vap}(T)$ by REFPROP[23] as a solid line.

pressures. Thus, it is likely that, for the force field approach used in this work, it is not possible to get a better description of all VLE properties of HFO-1234ze(E) at the same time, even when the LJ parameters are adjusted for this compound.

However, the good reproduction of both the vapor−liquid coexistence curve (VLCC) at higher and vapor pressure curve at lower temperatures results in an excellent estimate of the critical temperature, critical density, and normal boiling point, as they deviate by less than 0.3% from the reported experimental values.[4] The critical pressure though is overestimated by 6.6% due to the deviations between simulated vapor pressures and experimental data above 290 K.

However, for all that, the generally good prediction of the VLE properties of HFO-1234ze(E) without adjustment of the LJ parameters validates the predictive ability of the force field as well as the transferability of its parameters.

The same LJ parameters were then used to model the cis-HFO-1234ze, for which—to our best knowledge—no experimental information is available except for the normal boiling point reported by Mukhopadhyay et al.[42] Figures 2 and 3 also show the simulation results for the vapor pressures and saturated densities of HFO-1234ze in comparison with the data for the trans-isomer. From the simulation results, we estimated the normal boiling point of HFO-1234ze to be 283.6 ± 3.5 K, which is in excellent agreement with the experimental value[42] of 282.15 K. Also, the difference of $\Delta T_{b,exp}$ = 28 K (see Table 2) between the normal boiling point of HFO-1234ze(E) and HFO-1234ze is well reproduced by our simulation results ($\Delta T_{b,sim}$ = 28.7 K). Thus, our force field model seems to be well capable to reflect the different properties of the cis- and trans-isomer of HFO-1234ze. These results again also confirm the good transferability of our force field parameters. From our simulation results for the VLE of HFO-1234ze, we also estimated its critical properties. As shown by the comparison in Table 2, our data for T_c, p_c, and ρ_c are smaller than the values predicted by Brown et al.[42] Unfortunately, to our best knowledge, no experimental critical data are available for this compound to allow for an evaluation of the different estimates.

Vapor−Liquid Equilibria of HFO-1225ye(Z) and -1216. As described in section 2, we found that the FCM parameters used for HFO-1234yf, HFO-1243zf, and HFO-1234ze (with three to four fluorine atoms) result in simulated vapor pressures for HFO-1225ye(Z) that underestimate the experimental data by Singh,[41] whereas the simulated saturated liquid densities and heats of vaporization were higher than the experimental values. Thus, we slightly reduced the LJ parameter ε and increased σ for the FCM fluorine in this compound, resulting in the modified FCM^h parameter. We added the superscript h to indicate that this parameter should be used for the heavier fluoropropenes with at least five fluorine atoms. Figures 5 and 6

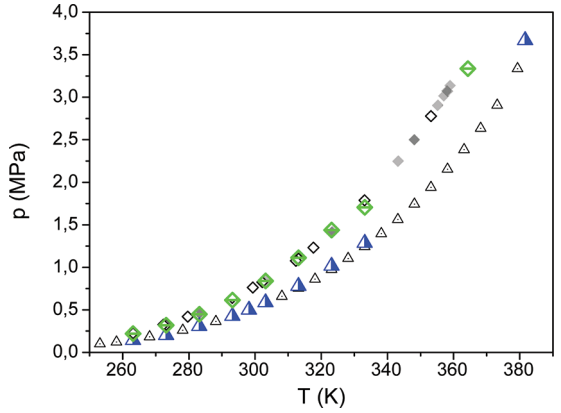

Figure 5. Comparison between Gibbs ensemble simulation results for the vapor pressures of HFO-1225ye(Z) (blue ◭) and HFO-1216 (green ◊) and experimental data (△[41] and ◇,[44] gray ◆,[8] respectively).

illustrate that the simulation results for the vapor pressures and the VLCC for HFO-1225ye(Z) using the modified FCM^h parameter are in good agreement with the experimental data.

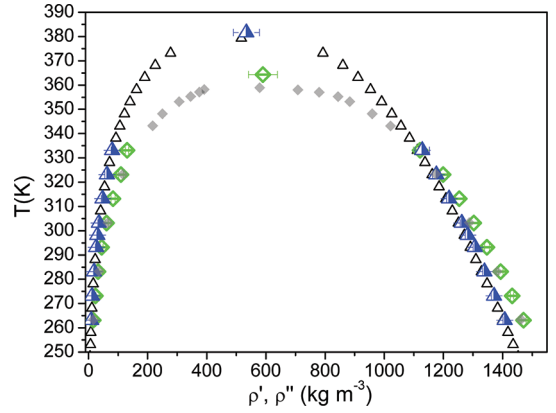

Figure 6. Comparison between experimental saturated liquid densities of HFO-1225ye(Z) (△[41]) and HFO-1216 (gray ◆[8]) and Gibbs ensemble simulation results for the saturated densities (blue ◭ and green ◊, respectively) obtained in this work.

From both our simulation results and experimental data for the vapor pressures and saturated densities, we estimated the critical properties of HFO-1225ye(Z), as described in section 3. The results are also given in Table 2. The derived T_c from simulation only deviates by 0.9% from the estimated critical temperature based on the experimental data,[41] whereas the simulated critical density overestimates the critical value from experimental data by 1.3%. The predicted critical pressure though is remarkably higher than the estimated value from experiment, as the simulations increasingly overestimate the experimental vapor pressures with increasing temperatures.

dx.doi.org/10.1021/jp300991t | J. Phys. Chem. B 2012, 116, 5744−5751

However, the good reproduction of the vapor pressure curve at lower temperatures results in an excellent estimate of the normal boiling point that only deviates by less than 0.3% from the interpolated experimental value.

Due to the lack of reliable experimental data and ambiguous vapor pressure correlations for HFO-1216 at that time, no efforts were made in our earlier work[25] to improve agreement between simulation and experiment or to adjust LJ parameters of our force field to experimental data for this compound. Only recently, additional experimental data for the vapor pressures and the saturated densities of HFO-1216 became available[8,44] that reveal that our simulation results published earlier underestimate the vapor pressures, whereas the saturated liquid densities are overestimated. Thus, we used the same FCM^h parameter, adjusted to improve agreement with experimental data for HFO-1225ye(Z), for new simulation studies on HFO-1216. The revised simulation results for the vapor pressure and saturated densities of this compound are also shown in Figures 5 and 6. The comparison with the experimental data[8,44] demonstrates the good reproduction of the VLE properties of this compound by the simulation with the modified FCM^h parameter. This also results in an improved prediction of the critical point, as the estimated critical temperature deviates from the experimental value[8] by only 1.5% (see Table 2). However, the overestimated critical temperature results in a predicted critical pressure that is by 6.5% higher than the experimental p_c value, whereas the critical density from simulation overestimates the experimental value by 1.9%. The experimental normal boiling point though is again well produced and falls within 0.5% of $T_{b,exp}$.

Once more, the generally good reproduction of the VLE properties of HFO-1216 using the same LJ parameters as for HFO-1225ye(Z) attest for the good transferability of our force field parameters.

Local Ordering in Liquid HFO-1234ze and HFO-1234ze(E). The cis- and trans-isomers HFO-1234ze and HFO-1234ze(E) exhibit pronounced diverse thermophysical properties with their normal boiling point differing by 28 K. Thus, we performed additional molecular dynamics studies for these compounds in order to investigate how their behavior might be affected by some local ordering. To get insight into the local structure and possible intermolecular hydrogen bonding, we analyzed the local structure of HFO-1234ze and -1234ze(E) in the liquid phase at 298.15 K and 2 MPa by radial distribution functions (RDFs).

In our earlier work,[24] we found that for HFO-1234yf neither the FCM-HC nor the FCT-HC RDF showed distinctive peaks, from which we concluded that no hydrogen bonding interactions occur in this compound. Thus, we determined different fluorine−hydrogen RDFs for HFO-1234ze and HFO-1234ze(E) to investigate if more pronounced hydrogen bond interactions exist in these compounds, and how they differ for the two isomers.

The comparison of the RDFs for the FCT and FCM fluorines of both compounds though reveals some differences in the local structures of the two isomers. Figure 7 illustrates that, for both compounds, the FCM-HC RDFs exhibit more pronounced first peaks than the RDFs of the FCM fluorine around the H1 hydrogen. In the FCM-HC RDF of HFO-1234ze(E), a first peak arises at 5.5 Å with a shoulder at 6.5 Å, and a second distinguishable peak appears at a distance of 9−10 Å. For the cis-isomer HFO-1234ze, the peaks in the FCM-HC RDF are more broadened, with a first peak that extends from a distance from 5 to 9 Å and has a maximum at 6.2 Å. The most noticeable curve in Figure 8 is the RDF of the FCT fluorine around the H1 hydrogen in HFO-1234ze, as it exhibits a first distinct maximum at 4.6 Å, i.e., at a smaller distance as all other fluorine−hydrogen RDFs. A second broad peak in this RDF extends from 7 to 11 Å. For the trans-isomer HFO-1234ze(E), the most notable RDF is the one of the FCT fluorine around the HC hydrogen, as it exhibits a broad split first peak with a first maximum at 5.5 Å and a second maximum at 7.1 Å.

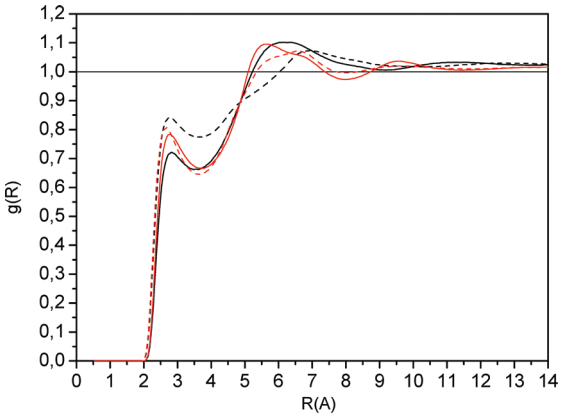

Figure 7. Radial distribution function for the FCM fluorine around the H1 (red - - -) and HC (red —) hydrogen in HFO-1234ze(E) and HFO-1234ze (black - - - and —, respectively) in the liquid phase at 298.15 K and 2 MPa.

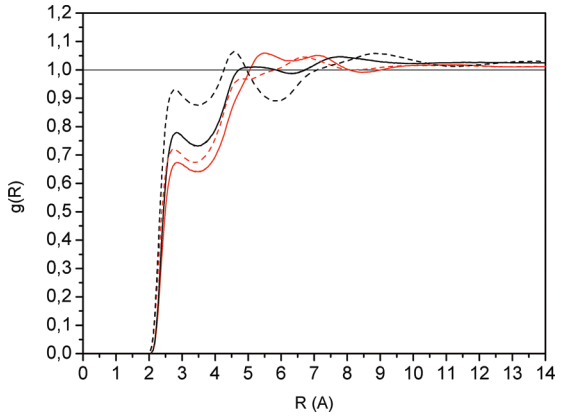

Figure 8. Radial distribution function for the FCT fluorine around the H1 (red - - -) and HC (red —) hydrogen in HFO-1234ze(E) and HFO-1234ze (black - - - and —, respectively) in the liquid phase at 298.15 K and 2 MPa.

Thus, there are some differences in the local ordering in the two isomers HFO-1234ze and HFO-1234ze(E), and their RDFs for the FCM and FCT fluorine around the H1 and HC in Figures 7 and 8 also show more distinctive peaks compared to HFO-1234yf. However, the peaks are still small and in general at higher distances and therefore indicate that hydrogen bonding interactions also only play a secondary role for HFO-1234ze and HFO-1234ze(E).

CONCLUSION

We have presented the extension of our transferable force field for molecular simulation studies of fluoropropenes to the compounds HFO-1234ze(E), HFO-1234ze, and HFO-1225ye(Z). The performance of the force field has been tested

dx.doi.org/10.1021/jp300991t | J. Phys. Chem. B 2012, 116, 5744−5751

by GEMC simulation studies of the vapor−liquid phase equilibria properties of these compounds.

Although no LJ parameters have been adjusted to improve agreement with experimental data, our force field yields good prediction for the VLCC, vapor pressures, normal boiling point, and critical properties of HFO-1234ze(E). Furthermore, the molecular model is able to reproduce the difference in the normal boiling point between the trans- and cis-isomer of this compound. These results validate both the predictive ability of the force field and the transferability of the parameters.

We found that the FCM parameter used to describe the compounds with up to four fluorines makes HFO-1225ye(Z) a too high-boiling compound. Thus, we derived a slightly modified FCM^h parameter for this compound, with which we are able to reproduce the vapor pressures and the VLCC for HFO-1225ye(Z) in good agreement with the experimental data.

We used the same FCM^h parameter to revise our simulation studies on HFO-1216. The revised simulation results for the vapor pressures and saturated densities are also in agreement with recent experimental results on the VLE properties of this compound.

We have additionally performed MD simulations to study the local ordering in liquid HFO-1234ze and -1234ze(E). From analyzing different hydrogen−fluorine RDFs, we conclude that no significant hydrogen bonding interactions occur in these compounds.

■ ASSOCIATED CONTENT

Supporting Information

The complete list of force field parameters (S1) as well as numerical results (S2) for the saturated densities, vapor pressures, and heats of vaporization from GEMC simulations for the compounds HFO-1234ze(E), HFO-1234ze, HFO-1225ye(Z), and HFO-1216. This material is available free of charge via the Internet at http://pubs.acs.org.

■ AUTHOR INFORMATION

Corresponding Author

*Phone: +49 531 391 2628. E-mail: G.Raabe@tu-bs.de.

Notes

The authors declare no competing financial interest.

■ REFERENCES

(1) Spatz, M.; Minor, B. HFO-1234yf, a low GWP refrigerant for MAC. *VDA Alternative Refrigerant Winter Meeting*, Saalfelden, Austria, 2008.

(2) Ikegami, T.; Aoki, K.; Lijima, K. New Refrigerant Evaluation results. *VDA Alternative Refrigerant Winter Meeting*, Saalfelden, Austria, 2008.

(3) McLinden, M. O.; Thol, M.; Lemmon, E. W. Thermodynamic Properties of trans-1,3,3,3-tetrafluoropropene [R1234ze(E)]: Measurements of Density and Vapor Pressure and a Comprehensive Equation of State. *International Refrigeration and Air Conditioning Conference*, Purdue, USA, 2010.

(4) Higashi, Y.; Tanaka, K. Critical Parameters and Saturated Densities in the Critical Region for trans-1,3,3,3-Tetrafluoropropene (HFO-1234ze(E)). *J. Chem. Eng. Data* **2010**, *55*, 1594−1597.

(5) Yamaya, K.; Matsuguchi, A.; Kagawa, N.; Koyama, S. Isochoric Specific Heat Capacity of trans-1,3,3,3 Tetrafluoropropene (HFO-1234ze(E)) and the HFO-1234ze(E) + CO_2 Mixtures in the Liquid Phase. *J. Chem. Eng. Data* **2011**, *56*, 1535−1539.

(6) Miyara, A.; Tsubaki, K.; Sato, N., Thermal Conductivity of HFO-1234ze(E) + HFC-32 Mixtures. *International Symposium on Next-generation Air Conditioning and Refrigeration Technology*, Tokyo, Japan, 2010.

(7) Subramoney, S. C.; Nelson, W. M.; Valtz, A.; Coquelet, C.; Richon, D.; Naidoo, P.; Ramjugernath, D. Pure Component and Binary Vapor-Liquid Equilibrium + Modeling for Hexafluoropropylene and Hexafluoropropylene Oxide with Toluene and Hexafluoroethane. *J. Chem. Eng. Data* **2010**, *55*, 411−418.

(8) Coquelet, C.; Ramjugernath, D.; Madani, H.; Valtz, A.; Naidoo, P.; Meniai, A. H. Experimental Measurement of vapor Pressures and densities of Pure Hexafluoropropylene. *J. Chem. Eng. Data* **2010**, *55*, 2093−2099.

(9) Patent Application US 2011/0260095 A1, MEXICHEM Amanco Holdings S.A. de C.V (2011).

(10) Patent Application WO 2011/073934 A1, ARKEMA France (2011).

(11) Patent US 7,825,081 B2, Honeywell International Inc. (2010).

(12) Patent US 7,959,825 B2, E.I. du Pont de Nemours and Company (2011).

(13) Patent Application WO 2010/002022 A1, Daikin Industries (2010).

(14) Patent Application US 2009/0158771 A1, Ineos Fluor Holdings Limited (2009).

(15) Hulse, R.; Singh, R.; Pham, H. Physical Properties of HFO-1234yf, *3rd IIR Conference on Thermophysical Properties and Transfer Processes of Refrigerants*, Boulder, USA, 2009.

(16) Di Nicola, G.; Polonara, F.; Santori, F. Saturated Pressure Measurement of 2,3,3,3-Tetrafluoroprop-1-ene (HFO-1234yf). *J. Chem. Eng. Data* **2010**, *55*, 201−204.

(17) Tanaka, K.; Higashi, Y. Thermodynamic properties of HFO-1234yf (2,3,3,3-tetrafluoropropene). *Int. J. Refrig.* **2010**, *33*, 474−479.

(18) Tanaka, K.; Higashi, Y.; Akasake, R. Measurement of the isobaric specific heat capacity and density of HFO-1234yf in the liquid state. *J. Chem. Eng. Data* **2010**, *55* (2), 901−903.

(19) Grebenkov, A. J.; Hulse, R.; Pham, H.; Singh, R. Physical Properties and Equation of State for trans-1,3,3,3-tetrafluoropropene, *3rd IIR Conference on Thermophysical Properties and Transfer Processes of Refrigerants*, Boulder, USA, 2009.

(20) Tanaka, K.; Takahashi, G.; Higashi, Y. Measurement of the vapor pressures and pρT- properties for trans-1,3,3,3-Tetrafluoropropene (HFO-1234ze(E). *J. Chem. Eng. Data* **2010**, *55*, 2169−2172.

(21) Tanaka, K.; Takahashi, G.; Higashi, Y. Measurement of the isobaric specific heat capacities for trans-1,3,3,3-Tetrafluoropropene (HFO-1234ze(E). *J. Chem. Eng. Data* **2010**, *55*, 2267−2270.

(22) Richter, M.; McLinden, M. O.; Lemmon, E. W. Thermodynamic properties of 2,3,3,3-Tetrafluoroprop-1-ene (R1234yf): Vapor Pressure and p-r-T Measurement and an equation of state. *J. Chem. Eng. Data* **2011**, *56*, 3254−3264.

(23) Lemmon, E. W.; Huber, M. L.; McLinden, M. O. REFPROP, Reference Fluid Thermodynamic and Transport Properties. NIST: Standard Reference Database 23, Version 9.0.

(24) Raabe, G.; Maginn, E. J. Molecular modeling of the vapor-liquid equilibrium properties of the alternative refrigerant 2,3,3,3-tetrafluoro-1-propene HFO-1234yf. *J. Phys. Chem. Lett.* **2010**, *1*, 93−96, 2675.

(25) Raabe, G.; Maginn, E. J. A Force Field for 3,3,3-fluoro-1-propenes, including HFO-1234yf. *J. Phys. Chem. B* **2010**, *114*, 10133−10142.

(26) Cornell, W. D.; Cieplak, P.; Bayly, C. I.; Gould, I. R.; Merz, K. M., Jr.; Ferguson, D. M.; Spellmeyer, D. C.; Fox, T.; Caldwell, J. W.; Kollmann, P. A. A Second Generation Force Field for the Simulation of Proteins, Nucleic Acids, and Organic Molecules. *J. Am. Chem. Soc.* **1995**, *117*, 5179−5197.

(27) Becke, A. D. Density-functional thermochemistry. III. The role of exact exchange. *J. Chem. Phys.* **1993**, *98*, 5648−5652.

(28) Lee, D.; Yang, W.; Parr, R. G. Development of the Colle-Salvetti correlation-energy formula into a functional of the electron density. *Phys. Rev. B* **1988**, *37* (2), 785−789.

(29) Godbout, N.; Salahub, D. R.; Andzelm, J.; Wimmer, E. Optimization of Gaussian-type basis sets for local spin density

functional calculations. Part I, Boron through neon, optimization technique and validation. *Can. J. Chem.* **1992**, *70*, 560−571.
(30) Frisch, M. J.; Trucks, G. W.; Schlegel, H. B.; Scuseria, G. E.; Robb, M. A.; Cheeseman, J. R.; Zakrzewski, V. G.; Montgomery, J. A.; Stratmann, R. E.; Burant, J. C.; et al. *Gaussian 98*, revision A.7; Gaussian, Inc.: Pittsburgh, PA, 1998.
(31) Breneman, C. M.; Wiberg, K. B. Determining Atom-Centered Monopoles from Molecular Electrostatic Potentials. The Need for High Sampling Density in Formamide Conformational Analysis. *J. Comput. Chem.* **1989**, *11*, 361−373.
(32) Panagiotopoulos, A. Z. Direct determination of phase coexistence properties of fluids by Monte Carlo simulation in a new ensemble. *Mol. Phys.* **1987**, *61*, 813−826.
(33) http://Towhee.sourceforge.net.
(34) Ewald, P. P. Die Berechnung optischer und elektrostatischer Gitterpotentiale. *Ann. Phys.* **1921**, *63*, 253.
(35) Frenkel, D.; Smit, B. *Understanding Molecular Simulation*; Academic Press: 1996.
(36) Martin, M. G.; Frischknecht, A. L. Using arbitrary trial distributions to improve intramolecular sampling in configurational-bias Monte Carlo. *Mol. Phys.* **2006**, *104*, 2439−2456.
(37) Smith, W.; Forester, T. R. The DL_POLY Molecular Simulation Package, http://www.cse.clrc.ac.uk/msi/software/DL_POLY.
(38) Hoover, W. G. Canonical dynamics. Equilibrium phase-space distributions. *Phys. Rev. A* **1985**, *31*, 1695−1697.
(39) Hoover, W. G. Constant pressure equations of motion. *Phys. Rev. A* **1986**, *34*, 2499−2500.
(40) Gmehling, J. Pure Compound data from DDB, 1983−2008.
(41) Singh, R. Personal communication, 2009.
(42) Mukhopadhyay, S.; Nair, N. K.; Tung, H. S.;. Van Der Puy, M.,Processes for synthesis of 1,3,3,3-tetrafluoropropene. U.S. Patent 7,345,209, 2008.
(43) Brown, J. S.; Zilio, C.; Cavallini, A. Thermodynamic properties of eight fluorinated olefins. *Int. J. Refrig.* **2010**, *33*, 235−241.
(44) Coquelet, C.; Valtz, A.; Naidoo, P.; Ramjugernatz, D.; Richon, D. Isothermal Vapor-Liquid Equilibrium Data for the Hexafluoropropylene (R1216) + Propylene System at Temperatures from (263.17 to 353.14) K. *J. Chem. Eng. Data* **2010**, *55*, 1636−1639.
(45) Kelkar, M. S.; Shiflett, M. B.; Yokozeki, A.; Maginn, E. J. Development of Force Fields for Hydrofluorocarbons. AIChE Annual Meeting, Philadelphia, USA, 2008.